

Synthesis, Characterization and Photoluminescence Study of Novel Sulfobetaine Polyelectrolytes

Nazia Tarannum · Hirdyesh Mishra · Meenakshi Singh

Received: 1 December 2009 / Accepted: 8 September 2010 / Published online: 5 October 2010
© Springer Science+Business Media, LLC 2010

Abstract A novel sulfobetaine copolymer is developed via polycondensation approach. The comonomers, melamine, condenses with a diketone, 5,5-dimethyl-1,3-cyclohexane (dimedone) to produce polyimine chain based on Schiff base chemistry. Dimedone-[N,N' melaminium] propane sulfonate copolymer crystals were obtained on treatment of the polyimine with sulfopropylating agent, 1,3-propane sultone with a crosslinker, di(ethylene glycol diacrylate) (DEGDA). This crosslinked sulfobetaine polymer yielded fine needle like single crystals and shows strong blue fluorescence and a weak green phosphorescence. Multi-exponential fluorescence decay function indicates the presence of different conformers both in solution and crystalline phase. This easy straightforward protocol for synthesis of crystalline, soluble, and luminescent polymer could prove to be a landmark in development of next generation smart functional materials.

Keywords Polyimine · Sulfobetaine · Crosslinking · Luminescence

Introduction

Ever since its discovery in 1864 by Hugo Schiff [1], this classical reaction has been a versatile tool in organic synthesis. The mechanism leading to the Schiff base is well understood. The dynamic nature of the imine bond formation has been also helpful in the build up of complex molecular architectures such as macrocyclic ligands [2] and interlocked molecules [3]. In view of the relevance of Schiff base chemistry and the search for nitrogen rich polymers in material science, melamine, a low cost industrial chemical has been reacted with dimedone, an aliphatic diketone, in a one-pot polycondensation approach. Herein, we report the synthesis of novel cross-linked polysulfobetaine crystals and their luminescence characteristics. The contributions from the leading research laboratories have demonstrated that the efficiencies of organic based devices can be competitive with those of their inorganic counterparts. Having highly extended π -conjugation systems in their main chain, polyimines and its derivatives are important semiconductor polymers for optical applications. With spin-casting, they are readily fabricated into large active areas in few micrometer range of thickness and exhibit a large efficiency for conversion between light and electricity. These polymers also possess the advantages of having efficient and versatile photoluminescence and electroluminescence.

In this study, we used the luminescent polyimines synthesized on the basis of Schiff base chemistry. Hitherto, the polybetaines consisting of iminium centres have not been reported as per our survey of the literature. Hence, a novel attempt has been made here keeping abreast of the relevance of Schiff base chemistry

N. Tarannum · M. Singh (✉)
Department of Chemistry, MMV, Banaras Hindu University,
Varanasi 221005, India
e-mail: meenakshi_s4@rediffmail.com

H. Mishra
Department of Physics, MMV, Banaras Hindu University,
Varanasi 221005, India
e-mail: hmishra@bhu.ac.in

and low cost diamines were reacted with dialdehydes, in a one-pot polycondensation approach. Polysulfobetaines show good biocompatibility [4–7], antibacterial properties and their utility for building bioinert coatings [8–10]. It is worth mentioning that the structure of sulfobetaine is similar to taurine, present in high concentration in animals and in trace concentration in plants [11]. Among the organic compounds showing photoluminescence in solid state, Schiff bases, especially N-salicylideneaniline and its derivatives (schiff bases) are on the forefront [12]. In recent reviews [13], it is noticeably concluded Schiff bases as one of the best selections to develop methodologies for selective preparation of photochromic crystals. They articulated that progress in the methodologies for the selective formation of photochromic crystals is the first important step for the development of optical devices; thus strategies for designing photochromic organic crystals promise to lead in a new direction of organic photochemistry and crystal engineering as well as materials science. Understanding the photoluminescence mechanism governing the efficiency and durability at a molecular level for polymers under operating conditions might provide important clues for an optimization of the chemical structure [14]. In the present paper easy straightforward protocol for synthesis of crystalline, soluble and luminescent polymer has been described,

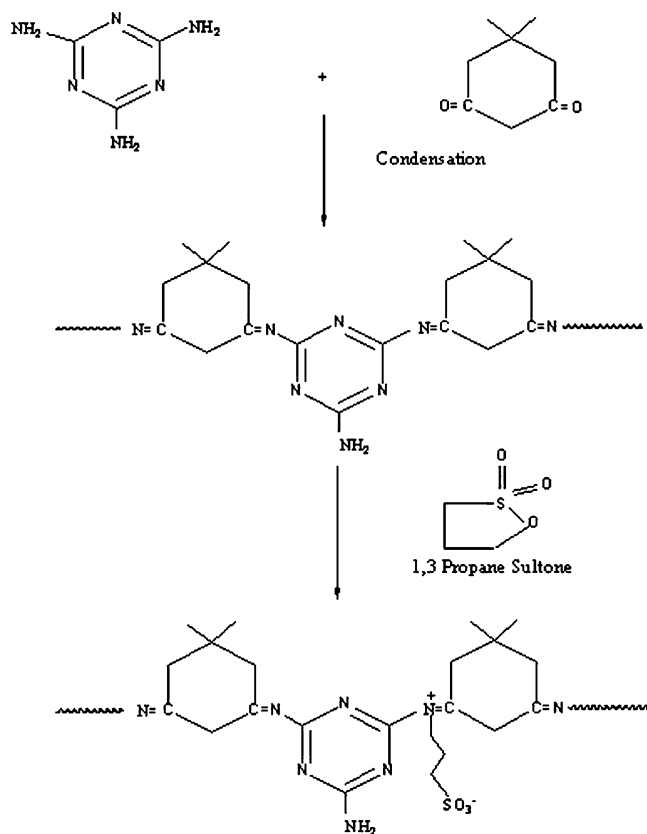


Fig. 1 Scheme of the polycondensation reaction for the polymer

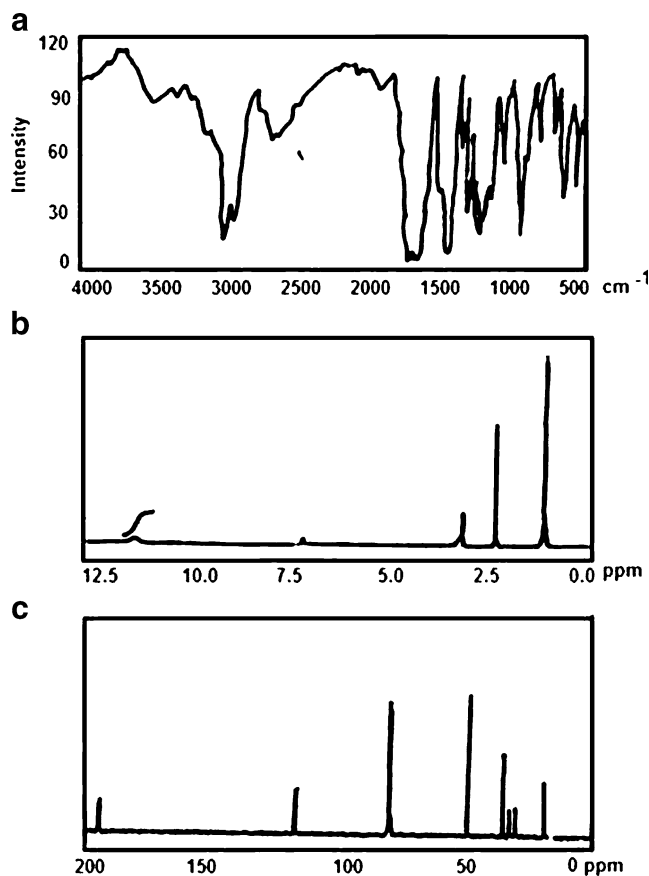


Fig. 2 a Infrared spectra in KBr, b ^1H NMR in CDCl_3 , c ^{13}C NMR in CDCl_3

which could prove to be a landmark in development of next generation smart functional materials in the field of photonics and electronics.

Experimental

Materials

The reagents melamine (pure) and dimedone (pure) were procured from Loba Chemie Pvt. Ltd. 1,3 propane sultone and di(ethylene glycol diacrylate) (DEGDA) were from Sigma Aldrich Co. Other chemicals were of analytical grade.

Synthesis

Dimedone-[N,N' Melaminium] Propane Sulfonate Copolymer

A solution of melamine [2.52 g (0.02 mol) in 25 ml DMSO] and dimedone [4.20 g (0.03 mol) in 25 ml DMSO] were prepared separately. The solutions were mixed and stirred at 45°C for 24 h. The colour of the reaction mixture

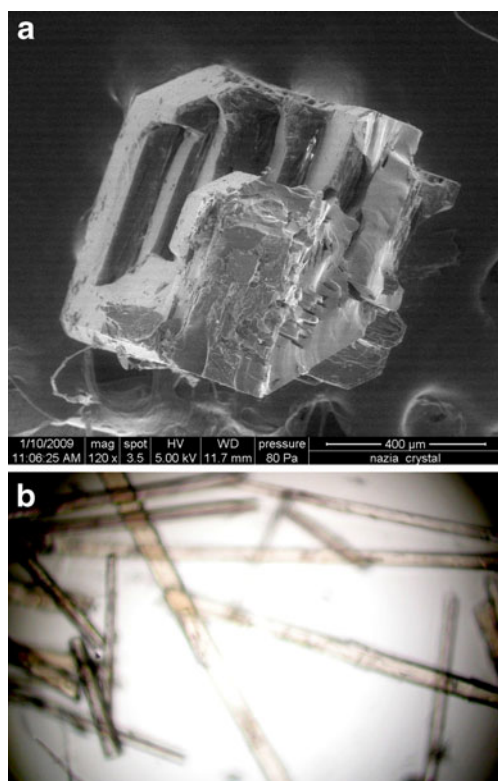
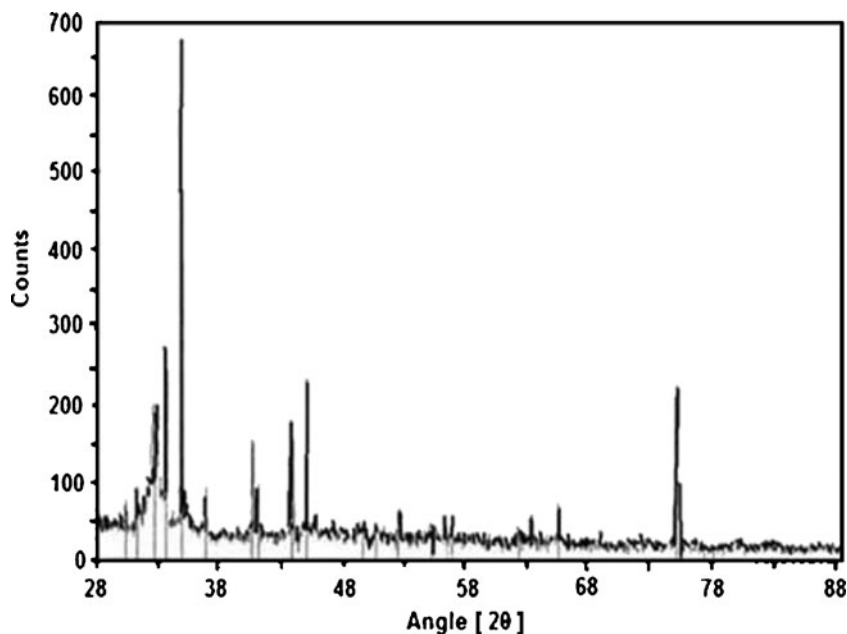


Fig. 3 **a** SEM (Scanning electron microscopy) image of crystalline polyzwitterion (120 \times magnification). **b** Phase contrast microscope image of the crystals (40 \times magnification)

turned reddish purple which was treated with 1,3-propane sultone [3.63 g (0.03 mol) in 10 ml DMSO] and left for overnight. Again this reaction mixture was subsequently treated with DEGDA [1.5 ml (14.5%)] and left for 48 h. Fine crystals were found on the surface of the reaction mixture

Fig. 4 Powdered X-ray Diffraction pattern showing the crystalline nature of the polymer



solution (yield 45%). The crystals were recrystallised in ethanol. mp 156°C. The purity of the sample was checked by TLC in solvent mixture: benzene 24 ml: acetic acid: 1 ml. As per the data collected from GPC, the polymeric crystal was found to have $M_w=12597$ and $M_n=11273$ PDI (Polymer Dispersity Index) of the sample was 1.11. The corresponding structure is shown in Fig. 1.

Characterization

FTIR (400–4000 cm^{-1} , KBr):

3456 (ν -NH), 2958 (asym. ν -CH₂), 2879 (sym ν -CH₂), 2629 (ν - Ar C=N), 1884 (ν - C=O), 1654 (ν - C=C), 1583 (ν - C=N), 1381, 1293, 1156 (asym, sym ν - SO₃⁻), 1248 (sym ν - COO), 1293 (asym ν -COO), 1085 (ν -C-O).

¹H NMR (300 MHz, CDCl₃, ppm):

δ 11.55 (2H, s, CH₂COO), 3.15 (2H, m, -CH₂ CH₂SO₃⁻), 2.28 (2H, s, -CH₂), 1.05 (6H, s, -C(CH₃)₂).

¹³C NMR (75 MHz, CDCl₃, ppm):

δ 189.0 (s, Ar C=N), 113.0 (2H, s, -C=N), 45.97 (s, -C(CH₃)₂), 31.75 (2H, t, -CH₂N), 29.47 (2H, t, CH₂S), 27.05 (2H, t, CH₂).

Equipments

Molecular weight determination of the crystal was done in THF using Autochro-GPC 1.0. The FT/IR of the sample was recorded with JASCO FT/IR 5300 in KBr from 400–4000 cm^{-1} . Thermogravimetric analyses (TGA/

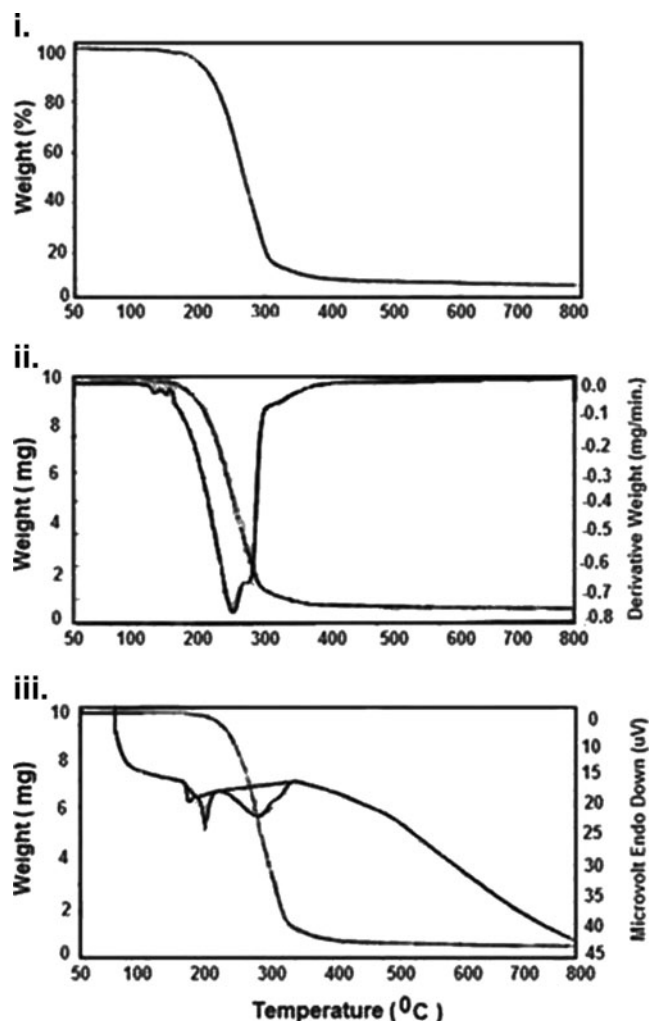


Fig. 5 (I) Thermogravimetric (TG) curve, (II) Differential Thermogravimetry (DTG) and (III) Differential Thermal Analysis (DTA) curve of the polymer

DTA) were performed using Perkin Elmer, Diamond TG/DTA at 10.0°C/min. Powder X-ray diffraction studies were done by PW1710 BASED. Scanning electron microscopy was performed by FESEM Quanta 200F at 5 KV in low vacuum. Potentiometric titrations were carried out on Systronics μ pH system. Conductometric titrations were carried on CM 180 conductivitymeter. Steady state absorption and fluorescence spectra were recorded on JASCO UV-550 spectrophotometer and JASCO FP-777 spectrofluorometer. Time domain fluorescence measurements were carried out via Horiba Jobin Yvon Tem Pro fluorescence lifetime system employing the time-correlated single photon counting (TCSPC) technique, with a TBX picosecond detection module. The excitation source was a pulsed LED source of wavelength 282 nm having maximum repetition rate 1.0 MHz and pulse duration 1.1 nanosecond (FWHM). The intensity decays were analyzed by decay analysis software (DAS) version 6.4 in terms of the multi-exponential model $I(t) = \sum_i \alpha_i \exp(-t/\tau_i)$, Where α_i are the amplitudes and τ_i are the decay times, $\sum_i \alpha_i = 1.0$.

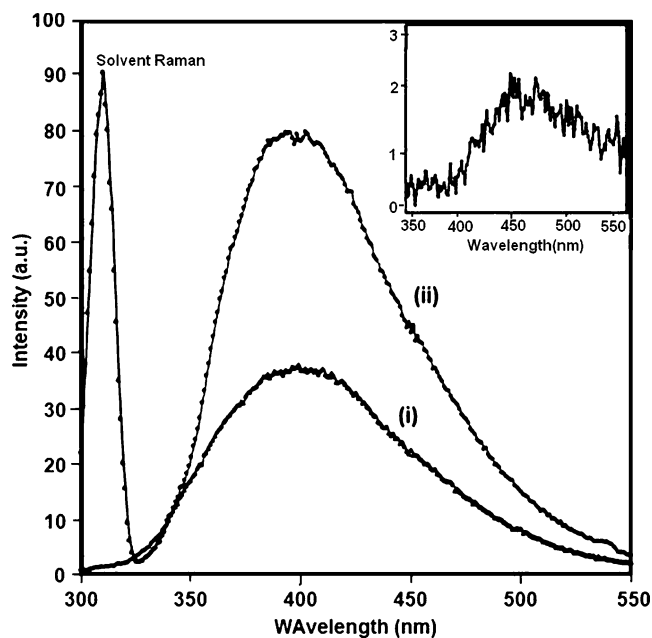


Fig. 6 Corrected fluorescence Spectra of crystalline powder excited by λ_{ex} (i) 270 nm and (ii) 310 nm. (Inset Phosphorescence spectra of polymer in excited by 270 nm)

Results and Discussion

Aldehydes and ketones react with primary amines and other ammonia derivatives to form imines, via the nucleophilic addition-elimination reaction. Melamine, a nitrogen rich,

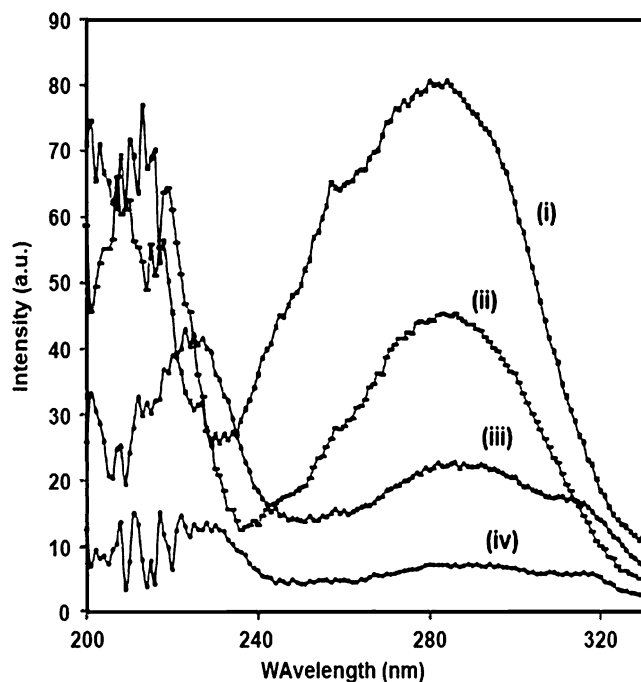


Fig. 7 Corrected Excitation Spectra of crystalline powder in between two quartz plate, with emission monitored at λ_{em} (i) 350 nm, (ii) 400 nm, (iii) 450 nm and (iv) 500 nm respectively

Table 1 Decay parameters of Polymer in ethanol and in crystalline state λ_{ex} 282 nm

[Conc.]	λ_{Ex} nm	τ_1 ns	$\alpha_1\%$	τ_2 ns	$\alpha_2\%$	τ_3 ns	$\alpha_3\%$			
10-4	400	1.40 \pm 0.05	90	6.97 \pm 0.07	10	–	–	–	1.372	10.621
	500	1.37 \pm 0.03	86	7.51 \pm 0.01	14	–	–	–	1.201	19.671
10-3	400	1.41 \pm 0.04	26	7.13 \pm 0.04	40	0.37 \pm 0.01	34	1.261	2.530	11.231
	500	1.45 \pm 0.07	20	7.74 \pm 0.03	52	0.32 \pm 0.09	28	1.182	3.648	9.687
solid	400	3.2 3 \pm 0.02	24	9.17 \pm 0.04	44	0.49 \pm 0.01	32	1.102	2.131	7.144
	500	3.10 \pm 0.05	21	8.76 \pm 0.07	52	0.42 \pm 0.04	27	1.301	3.219	10.121

triazine derivative (2,4,6-triamino-s-triazine) was condensed with a diketone, 5,5-dimethyl-1,3-cyclohexane (dimedone). In this mechanism, the non-bonded electrons on nitrogen causes water to be eliminated and further subsequent loss of a proton from the resulting protonated imine forms a stable imine. In general, imines are only stable enough to isolate if either the C or N of the imine double bond bears an aromatic substituent and/ or nitrogen atom carries an electronegative group. The electronegative substituent can participate in delocalization of the imine double bond and raises the energy of the LUMO, making it less susceptible to nucleophilic attack. Here, the aromatic group from the melamine facilitates the delocalization of the probable charge centres on the C atom of imine groups.

The resulting polyimine was subsequently treated with 1,3-propane sultone followed by DEGDA as a crosslinker. Upon crosslinking, fine crystals of the resulting polyiminosulfobetaine were obtained. 1,3-propane sultone, a sulfoalkylating agent, in their reaction with nucleophiles, quaternized the imine centres of poly-schiff base, resulting in zwitterionic centres along the polymeric chains (Fig. 1). The sulfopropyl

groups are introduced by reaction of nucleophiles with commercially available 1,3 propane sultone [15].

The infrared, ^1H NMR, ^{13}C NMR spectra are shown in Fig. 2. The successful conversion of the functional groups initially present in the monomers was confirmed by FTIR. The absorption due to imine group appears at 1583 cm^{-1} and those for sulfonate group at 1381 , 1293 and 1156 cm^{-1} . Chemical shifts were referred to the CDCl_3 triplet centered at 77.00 ppm for ^{13}C NMR and the 7.26 ppm residual CHCl_3 peak for ^1H NMR. The presence of imine was confirmed by peak at 113 ppm in ^{13}C NMR spectra. The other remarkable peaks shown by ^{13}C NMR spectra are at δ 189 (singlet) of aromatic $\text{C}=\text{N}$ (melamine), δ 45.97 (singlet) of $-\text{C}(\text{CH}_3)_2$ (dimedone), δ 31.75 (triplet) of CH_2N (pendant group), δ 29.47 (triplet) of $-\text{CH}_2\text{S}$ and δ 270.5 (triplet) of $-\text{CH}_2$ group.

While the ^1H NMR spectra gave the corresponding peaks at δ 11.55 (singlet) of $-\text{CH}_2\text{COOH}$ (DEGDA), δ 3.15

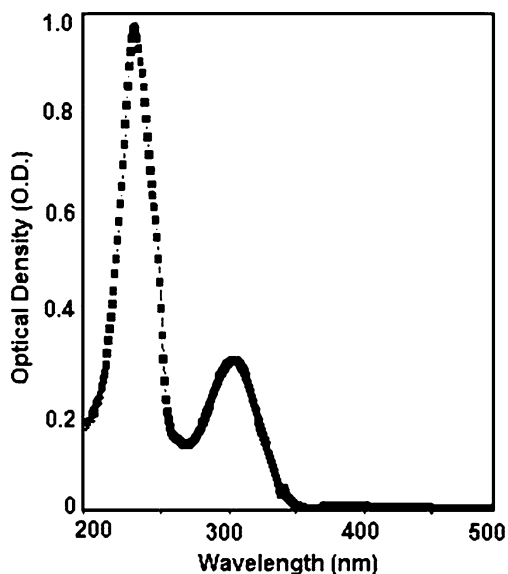


Fig. 8 Absorption spectrum of the crystal in ethanol at concentration $0.11 \times 10^{-4}\text{ g/ml}$

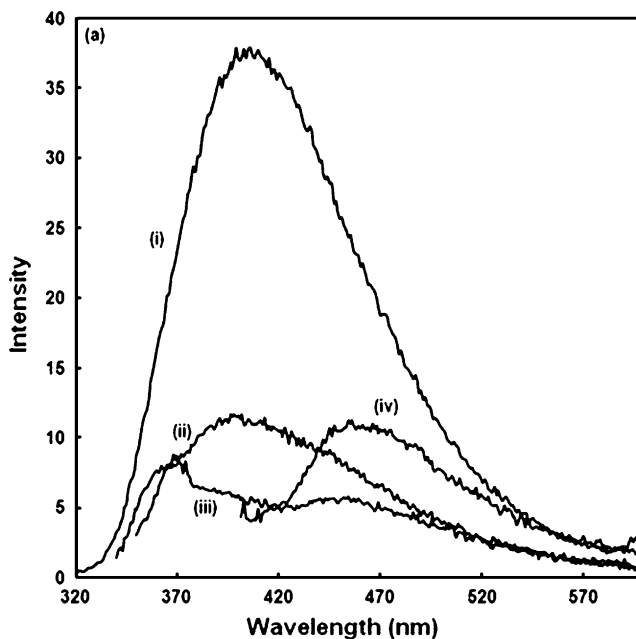


Fig. 9 a Corrected fluorescence Spectra of polymer in ethanol excited by λ_{ex} (i) 270 nm, (ii) 290 nm, (iii) 350 nm and (iv) 400 nm

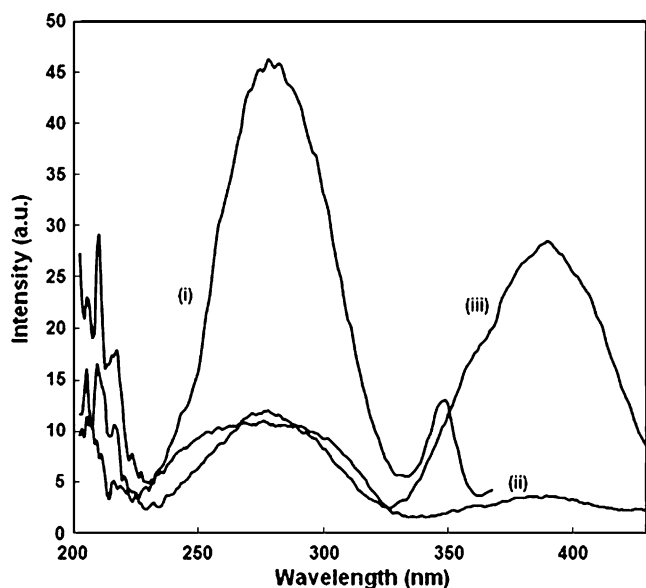


Fig. 10 Corrected Excitation Spectra of polymer in ethanol, with emission monitored at λ_{em} (i) 370 nm, (ii) 450 nm and (iii) 500 nm respectively

(multiplet) of $-\text{CH}_2\text{CH}_2\text{SO}_3^-$ (pendant group) and δ 1.05 (singlet) of $-\text{C}(\text{CH}_3)_2$ (dimedone).

Scanning electron microscopy (SEM) image is shown in Fig. 3(a). Long needles of single crystals were seen at lower magnification $40\times$ (Fig. 3(b)). The crystal of polymer was studied for its powdered X-ray diffraction pattern. The peaks in the diffraction pattern were sharp and the ratio of the half height width to diffraction angle is less than 0.35 designating the polymeric sample as crystal (Fig. 4). The particle size can be calculated from Scherrer formula as

$$L\theta = \frac{k\lambda}{\beta \cos \theta} \quad (1)$$

k = constant that varies with the method of taking the breadth, λ is the wavelength of incident X-rays, θ is the centre angle of the peak. Average size of the crystal from powdered XRD was calculated to be 434.99 Å. Size of the crystal with 100% relative intensity is 513.78 Å.

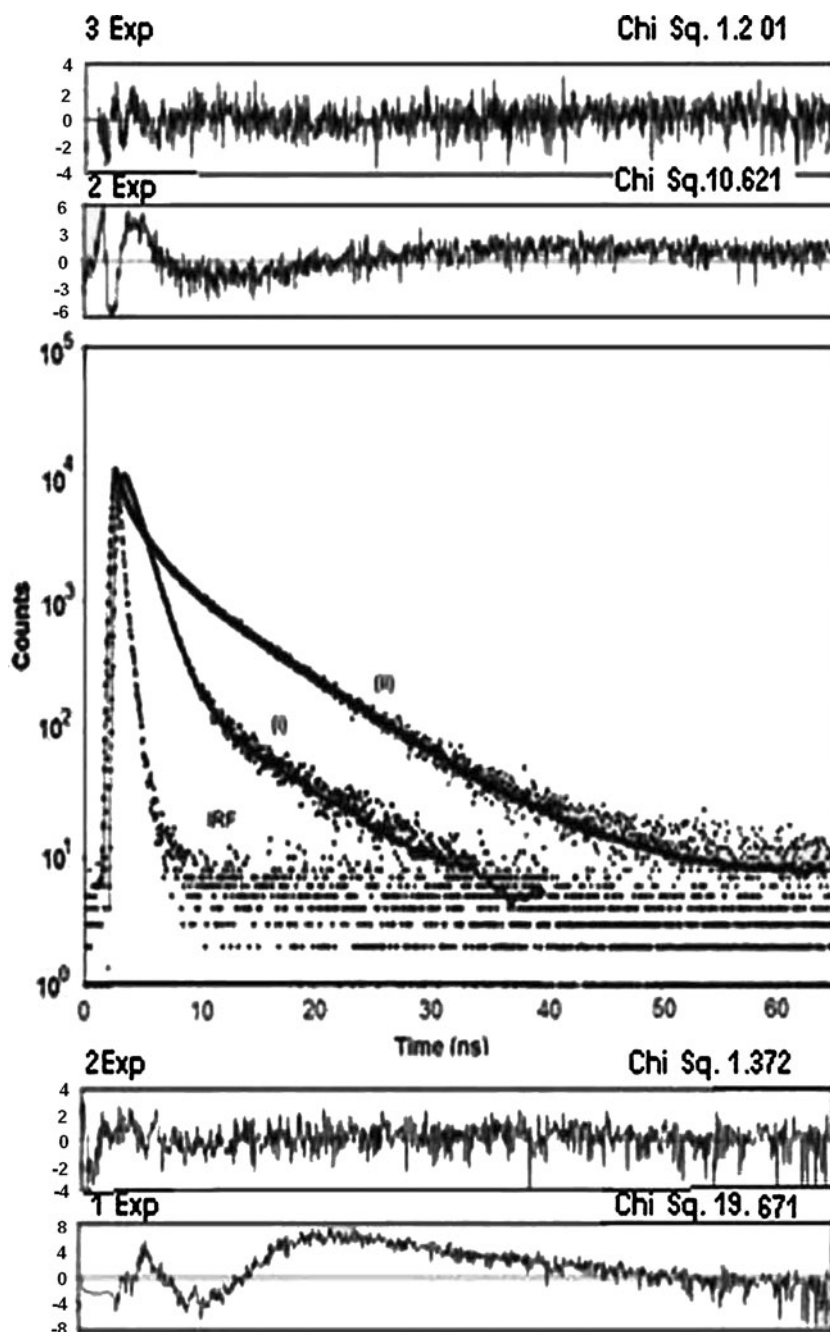
While examining the mp of the polymer, some unusual phenomenon was observed. The thermogravimetric (TG) curve shows that the compound is stable at $<200^\circ\text{C}$, afterwards it gradually decomposes up to 310°C and ~ 5 – 10% residue remains are left (Fig. 5). While examining mp, the polymer transformed into molten state at 156°C and on cooling it became white solid, physically appearing as fused material. On further heating, it again melted and on cooling again, it turned out to be white solid. The initial degradation temperature is 152°C , at 269°C , 20% weight loss is observed and at 310°C , 50% wt is lost. On close circumspection of the TGA curves, in the derivative weight vs temperature plot, a kink is observed at $\sim 150^\circ\text{C}$ and the complete decomposition

starts at $\sim 200^\circ\text{C}$ with another hump at $\sim 330^\circ\text{C}$, $\sim 360^\circ\text{C}$ before reaching to zero of the curve. Largely, the decomposition appears a one-step process but the kinks describe some kind of chain movements and functional group interactions resulting to weight change as observed in derivative weight plot. The picture becomes clearer in DTA curves. It shows that crystals are in molten state at 180°C . Three endothermic peaks are seen in the Fig. 5. A very small peak at 152.9°C represents a slight change in functional group orientations involving a heat of ~ 15 J/g. A second sharp peak at 180°C may be due to small movement of chains and cross-links with a little more heat change of 51 J/g. The major decomposition is observed in the large peak of 269°C where the whole polymeric chain is decomposed with 254 J/g heat change.

The corrected fluorescence spectrum of solid crystalline copolymer in between two quartz plate excited by 270 nm and 310 nm in frontal direction and is shown in Fig. 6. It shows a broad fluorescence ranging from 300 to 550 nm with maxima at 400 nm. Intensity of 270 nm excitation gives larger intensity with respect to 310 nm excitation. Further, the excitation spectra of the emission band monitored at different wavelength are given in Fig. 7. Fluorescence decay measurement of crystal samples show triple exponential decay with decay time 3.2 ns, 9.17 ns and 0.49 ns with nearly 24%, 44% and 32% contribution as given in Table 1. Thus result indicates that the crystal sample contain at least three different kind of conformers. Further the crystals also show a weak after glow (phosphorescence) at 475 nm in the in the order of few seconds.

To understand the possibility of different conformers in crystalline state, solvent phase studies of copolymer has been undertaken in ethanol at different concentration. Fig. 8 shows the absorption spectrum of the polysulfobetaine (conc. 10^{-4} M) in ethanol. It shows absorption maximum at 232 nm, 304 nm and a very weak band at 400 nm respectively. The average molar absorptivity coefficient (ϵ) is $28.05 \text{ cm}^{-1} \text{ g}^{-1} \text{ L}$. The molar absorptivity for the absorption at $\lambda_{max}=232$ nm is 42. This absorption maxima is due to $n \rightarrow \pi^*$ transition of the chromophore and that for the second absorption ($\lambda_{max}=304$ nm) is 15. This absorption is assigned to $n \rightarrow \pi^*$ transition of the second chromophoric group. It is difficult to strictly assign the chromophoric groups. The second transition at $\lambda_{max}=304$ nm may be assigned to the carbonyl groups present in the crosslinker DEGDA. The electronic transition responsible for absorption at 232 nm perhaps assigned to the imine groups of the polymer chain. Corrected fluorescence spectra corresponding to these absorption bands of the polymer molecule in ethanol are shown in Fig. 9. It appears that on 270 nm excitation, fluorescence maximum was observed at 420 nm. On further excitation by 290 nm, fluorescence intensity of the band decreases but further

Fig. 11 Overlapped decay curve of polymer in ethanol at (i) 400 nm and (ii) 500 nm. $\lambda_{ex}=282$ nm



excitation by longer wavelength 350 nm, emission intensity of 420 nm band decreases and a new band appears at 470 nm. Intensity of this 470 nm band increases by 400 nm excitation. To understand the origin of these emission bands, excitation spectrum of the molecule in ethanol are undertaken at different emission wavelength and are shown in Fig. 10. On monitoring the emission at 370 nm, excitation maximum observed at 290 nm while on monitoring the emission spectra at 420 nm and 470 nm, excitation maximum was observed at 290 nm and 390 nm respectively. The intensity of 390 nm band increases at red edge of the emission band. The difference in excitation

spectra with respect to absorption spectra confirming the presence of two absorbing moieties. In excitation spectrum, the luminescence intensity is measured at a fixed wavelength while the excitation wavelength is varied. Since a fluorescence emission is generated by absorption of radiation to create excited states, an excitation spectrum is identical to an absorption spectrum recorded under similar experimental conditions. Phosphorescence is a quasistable electron excitation state involving a change of spin system (intersystem crossing) which decays only slowly. It is similar to fluorescence but the species is excited to a metastable state from which a transition to the initial state is forbidden. The

chromophoric groups present in the polymer are showing intersystem crossing in which the spin of an excited electron is reversed and a change in multiplicity of the molecule results. Generally, intersystem crossing is common in those systems where heavy atoms are present [20], so the workers in this field have attempted π -conjugated systems with metal complexes where spin-orbit coupling is strong. In solution no phosphorescence were detected due to increase of non radiative transition.

To understand the dynamics of the polymer fluorescence, time domain fluorescence measurements were undertaken at different concentrations and at different wavelengths both in solution and crystalline state as given in Table 1. Overlapped analysed decay curve of the polymer in ethanol at 10^{-3} M and 10^{-4} M are given in Fig. 11. At lower concentration double exponential decay curve is observed throughout the emission profile with decay components 1.40 ns and 6.97 ns. The percentage of shorter decay component is higher (85%) and the amplitude of longer decay component is low (15%). On increasing the concentration, fluorescence decay started to fit in Triple exponential function along with an additional decay component of 0.37 ns. It is also observed that the amplitude of shorter decay time decreases while the amplitude of longer decay time increases with increase in concentration. The distribution of residual and chi-square for both the concentrations (10^{-4} and 10^{-3} M) decay curves are given below and above of the overlapped decay curve respectively. The results also indicate that at lower concentration there are two emitting conformers of polymer in solution when on increasing the concentration the oligomerization takes place and an additional decay component appears.

Conclusion

In summary, we have presented a novel synthetic protocol for the design and build up of crosslinked polyelectrolytes based on Schiff base chemistry. Several unique characteristics make the materials promising candidates for potential applications in material science: (i) the proposed condensation approach leads to materials with fluorescing and phosphorescing behaviour, (ii) cheap materials are obtained due to the low price starting compounds and the easy way of synthesis, whereas other synthetic pathways often rely on costly reaction conditions and or building blocks [21–25], (iii) no catalyst is needed for the formation of the polymeric networks, so the materials are not contaminated with inorganic remains or byproduct as this is observed in other systems [26–30], (iv) the use of melamine as amine component leads to materials with a high nitrogen content, (v) a novel material for developing LEDs and electrically driven lasers.

Acknowledgements The financial support by Department of Science and Technology [SR/S2/CMP-65/2007] is gratefully acknowledged. Authors acknowledge Prof.GVS Sastry (SEM), Dr. B Ray (GPC) and Dr. S Pant with his research group for their kind help. Authors are also highly thankful to Prof. C.D. Geddes, Director Institute of fluorescence, UMBC, Baltimore MD, USA for some of the time domain fluorescence measurements.

References

- Schiff H (1864) Mittheilungen aus dem Universitätslaboratorium in Pisa: Eine neue Reihe organischer Basen Liebigs Justus. Ann Chem 131:118–119
- Borisova NE, Reshetova MD, Ustynuk YA (2007) Metal-free methods in the synthesis of macrocyclic schiff bases metal-free methods in the synthesis of macrocyclic schiff bases. Chem Rev 107:46–79
- Rowan SJ, Stoddart JF (1999) Thermodynamic synthesis of rotaxanes by imine exchange. Org Lett 1:1913–1916
- Yuan J, Zhang J, Zang X, Shen J, Lin S (2003) Improvement of blood compatibility on cellulose membrane surface by grafting betaines. Colloids Surf B 30:147–155
- Kitano H, Tada S, Mori T, Takaha K, Gemmei-Ide M, Tanaka M, Fukuda M, Yokoyama Y (2005) Correlation between the structure of water in the vicinity of carboxybetaine polymers and their blood-compatibility. Langmuir 21:11932–11940
- West SL, Salvage JP, Lobb EJ, Armes SP, Billingham NC, Lewis AL, Hanlon GW, Lloyd AW (2003) The biocompatibility of crosslinkable coatings containing sulfobetaine and phosphobetaine. Biomaterials 25:1195–1204
- Zhang Z, Chen S, Chang Y, Jiang S (2006) Surface grafted sulfobetaine polymers via atom transfer radical polymerization as superlow fouling coatings. J Phys Chem B 110:10799–10804
- Lewis AL, Cumming ZL, Goreish HH, Kirkwood LC, Tolhurst LA, Stratford PW (2001) Crosslinkable coatings from phosphorylcholine based polymers. Biomaterials 22:99–111
- Lowe AB, Vamvakaki M, Wassall MA, Wong L, Billingham NC, Armes SP, Lloyd AW (2000) Well defined sulfobetaine based statistical copolymers as potential antibioadherent coatings. J Biomed Mater Res 52:88–94
- Salloum DS, Olenych SG, Keller TCS, Schlenoff JB (2005) Vascular smooth muscle cell on polyelectrolytes multilayers: hydrophobicity directed adhesion and growth. Biomacromolecules 6:161–167
- Huxtable RJ (1992) Physiological actions of taurine. Physiol Rev 72:101–163
- Amimoto K, Kawato T (2005) Photochromism of organic compounds in the crystal state. J Photochem Photobiol C Photochem Rev 6:207–226
- Hadjoudis E, Mavridis IM (2004) Photochromism and thermochromism of Schiff bases in the solid state: structural aspects. Chem Soc Rev 33:579–588
- Mishra H (2006) Photo-induced excited State relaxation of hydroxy naphthoic acids in polymers. J Phys Chem B 110 (19):9387–9396
- Roberts W, Liams WLD (1987) Sultone chemistry. Tetrahedron 43:1027–1062
- Schmitt KD (1995) Surfactant-mediated phase transfer as an alternative to propanesultone alkylation. Formation of a new class of zwitterionic surfactants. J Org Chem 60:5474–5479
- Gautun OR, Carlsen PHJ, Maldal T, Vikane O, Gilje E (1996) Selective synthesis of aliphatic ethylene glycol sulfonate surfactants. Acta Chem Scand 50:170–177

18. Flanagan JH, Khan SH, Menchen S, Soper SA, Hammer RP (1997) Functionalized tricyanocyanine dyes as near-infrared fluorescent probes for biomolecules. *Bioconjugate Chem* 8:751–756
19. Carrea G, Ottolina G, Riva S, Danieli B, Lesma G, Palmisano G (1988) Alkylation of adenine, adenosine, and nad⁺ with 1, 3-propanesultone. synthesis of n6-(3-sulfonatopropyl)-nad⁺, a new nad⁺ derivative with substantial coenzyme activity. *Helv Chem Acta* 71:762–772
20. Misra V, Mishra H (2008) Photoinduced proton transfer coupled with energy transfer: Mechanism of sensitized luminescence of terbium ion by salicylic acid doped in polymer. *J Chem Phys* 128:244701–244707
21. Han SS, Furakawa H, Yaghi OM, Goddard WA (2008) Covalent organic frameworks as exceptional hydrogen storage materials. *J Am Chem Soc* 130:11580–11581
22. McKeown NB, Budd PM (2006) Polymers of intrinsic microporosity (PIMs): organic materials for membrane separations, heterogeneous catalysis and hydrogen storage. *Chem. Soc Rev* 35:675–683
23. Mackintosh HJ, Budd PM, McKeown NB (2008) Catalysis by microporous phthalocyanine and porphyrin network polymers. *J Mater Chem* 18:573–578
24. Cote AP, Benin AI, Ockwig NW, Koeffe MO, Matzger AJ, Yaghi OM (2005) Porous, crystalline, covalent organic frameworks. *Science* 310:1166–1170
25. Jiang JX, Su F, Trewin A, Wood CD, Campbell NL, Niu H, Dickinson C, Ganin AY, Rosseinsky MJ, Khimyak YZ, Cooper AI (2007) Conjugated microporous poly(aryleneethynylene) networks. *Angew Chem Int Ed* 46:8574–8578
26. Wood C, Tan B, Trewin A, Niu H, Bradshaw D, Rosseinsky MJ, Khimyak YZ, Campbell NL, Kirk R, Stockel E, Cooper AI (2007) Hydrogen storage in microporous hypercrosslinked organic polymer networks. *Chem Mater* 19:2034–2048
27. Schmidt J, Weber J, Epping JD, Antonietti M, Thomas A (2009) Microporous Conjugated poly(thienylene arylene) networks. *Adv Mater* 21:702–705
28. Kuhn P, Antonietti M, Thomas A (2008) Porous, covalent triazine-based frameworks prepared by ionothermal synthesis. *Angew Chem Int Ed* 47:3450–3453
29. Davankov VA, Tsyurupa MP (1990) Structure and properties of hypercrosslinked polystyrene—the first representative of a new class of polymer networks. *React Polym* 13:27–42
30. Rose M, Bohlmann W, Sabo M, Kaskel S (2008) Element–organic frameworks with high permanent porosity. *Chem Commun* 2462–2464